ELSEVIER

Polymer 40 (1999) 6113–6124

polymer

The stress and sonic modulus versus strain curve of polymer fibres with yield

J.J.M. Baltussen[a,*], M.G. Northolt[b]

[a]*Akzo Nobel Central Research, Zutphenseweg 10, P.O. Box 10, 7400 AA Deventer, The Netherlands*
[b]*Akzo Nobel Central Research, Velperweg 76, P.O. Box 9300, 6800 SB Arnhem, The Netherlands*

Received 11 August 1997; accepted 12 January 1998

Abstract

The stress vs. strain curve with yield and the sonic modulus vs. strain curve of fibres of linear polymers below the glass transition temperature are modelled by the continuous chain model in combination with a simple yield model. It is supposed that yield of polymer fibres is due to shear deformation of the domains. The yield model is based on a critical shear yield strain. A good agreement between the experimental tensile and sonic modulus vs. strain curves and the theoretical curves has been obtained for a selection of poly(*p*-phenylene terephthalamide) and poly(ethylene terephthalate) fibres. © 1999 Elsevier Science Ltd. All rights reserved.

Keywords: Polymer fibres; Stress–strain curves; Sonic modulus

1 . Introduction

The stress vs. strain curve of polymer fibres below their glass transition temperature is characterised by a more or less pronounced yield at about 0.005–0.025 strain. Some typical stress vs. strain curves have been depicted in Fig. 1. Below the yield point the deformation of the fibre is almost elastic. Above the yield point the deformation of the fibre is partly permanent. In the classical theory, yield is described by a yield criterion. In its most general form the yield criterion is a function of all components of the applied stress, which reaches a critical value at the onset of yield of the material. Originally this yield theory was developed for the description of the yield of crystalline materials like metals. Although the yield behaviour of polymers depends on the temperature and the time scale of the deformation, Ward showed that the classical ideas of plasticity are relevant to the yield of polymers as well [1]. Underlining the common features of the yield of polymers, he remarks that the same yield behaviour can be found for all polymer materials, independently of their chemical nature and physical structure. Above the yield point slip bands and kink bands have been observed for both polymer and crystalline materials which is an indication for the similarity of the yield processes in polymer and crystalline materials on a mesoscopic scale. For crystalline materials it is generally accepted that on a molecular scale the plastic deformation is due to motion of dislocations. For crystalline polymers, in particular for highly crystalline polyethylene, it has been shown that plastic deformation can be explained by motion of dislocations as well [2–5]. Mott and Argon argue that in case of amorphous polymers the deformation mechanism may be more complicated [6,7]. However, the similarity of the yield of polymers and crystalline materials on macroscopic and mesoscopic level justifies the use of the same phenomenological continuum theory for the modelling of the stress vs. strain behaviour of polymer fibres.

A simple criterion for the yield of isotropic polymers is the Tresca yield criterion, which states that yield occurs when the maximum shear stress reaches a critical value [8]. The Coulomb yield criterion supposes that the critical shear yield stress is a linearly increasing function of the stress normal to the shear plane [9]. Another well-known yield criterion is the von Mises yield criterion which relates the occurrence of yield to a critical value of the second invariant of the deviatoric stress tensor [10]. The logical extension of the Tresca yield criterion for anisotropic materials is the resolved shear-stress law of Schmid [11]. This yield criterion states that yield occurs when the resolved shear stress in a slip direction reaches a critical value, i.e. the direction of the shear deformation is determined by the structure of the material. On a microscopic scale polymers are not isotropic at all. Due to the presence of the covalent

* Tel.: +31-570-679222; fax: +31-570-624113.
E-mail address: joop.baltussen@dvt.akzonobel.com (J.J.M. Baltussen)

PII: S0032-3861(99)00194-9

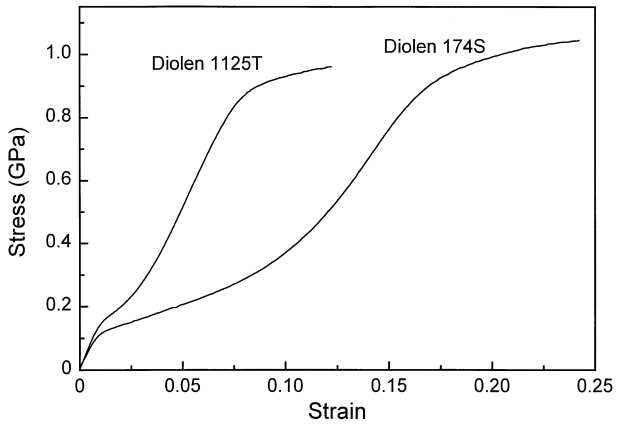

Fig. 1. Typical stress vs. strain curves of two PET fibres.

chains, the local mechanical properties are highly anisotropic. Young proposed a critical resolved shear stress model for the yield of highly oriented polyethylene [4,5]. With this model he explained the results of compression experiments in which the angle between the chain orientation and the compression direction was about 45°.

The elastic deformation of polymer fibres has been described previously by the continuous chain model [12,13]. It has been shown in Ref. [12] that the curve of the elastic or sonic modulus vs. the strain can be described by the continuous chain model below and above the yield point, which implies that the same mechanism governs the deformation above and below the yield point. The continuous chain model for the elastic deformation of polymer fibres describes the deformation of the fibre as the average deformation of small perfectly oriented domains. It shows that only the extension of the chain and the shear of adjacent chains contribute to the tensile deformation of the fibre. This description of the deformation of a fibre suggests that the position of the yield point can be understood from Schmid's law for the resolved shear yield stress applied in the system of local symmetry. At a critical value of the resolved shear stress, local debonding of the secondary bonds between adjacent chains occurs, resulting in a permanent displacement of adjacent polymer chains and thus a permanent shear deformation of the domain. It has been shown by Northolt and Baltussen that the yield strain predicted by this yield criterion agrees well with the experimentally determined yield strain of polymer fibres and sheets. In particular it explains the position of the yield point as a function of the orientation parameter [14]. This model for the yield emphasizes once more the essential role of the orientation distribution in the mechanical properties of polymers. From the analysis of the compression strength of polymer fibres it results that the yield strain in compression is approximately equal to the yield strain in extension. The continuous chain model can not be used for the calculation of the yield point of oriented polymers at an arbitrary stress. It is only valid if the deformation is determined by average projection length of the polymer chains. So, the applied stress should be in the direction of the average orientation, or at a small angle with this direction. For example it does not predict the yield point for a stress perpendicular to the axis of an oriented fibre.

In this article it will be shown that the stress vs. strain curve and the modulus vs. strain curve of polymer fibres can be described by the continuous chain model in combination with a simple yield assumption based on a critical shear yield strain. First the theory for the deformation of a yielding fibre is developed. It will be shown that the plastic deformation of a domain is a simple shear deformation. It is proposed that the plastic shear deformation is a function of the elastic shear deformation. Next the nature of the yield and the applicability of the continuous chain model is studied. Finally the functional dependence of the plastic deformation is examined and the calculated curves compared with the observed curves of poly(ethylene terephthalate) (PET) and poly(*p*-phenylene terephthalamide) (PpPTA) fibres. In the last section it will be shown that the stress vs. strain curve and the sonic modulus vs. strain curve can be described simultaneously by the equations for the yielding fibre. Preliminary results of this model have been published earlier [15].

2. Theory of the deformation of a yielding fibre

2.1. Introduction

It is supposed that the deformation of a fibre is composed of an elastic and a permanent contribution which can be both reduced to the local elastic and permanent deformation. For the description of the deformation of the fibre the continuous chain model is used. The continuous chain model has been described in Refs. [12,13]; a summary of the model is given next. The fibre consists of long and continuous chains which do not break during the deformation. Along the chain small linear segments of equal length are considered. The angle between the undeformed chain segment and the fibre axis is denoted by Θ, after a deformation the angle is denoted by θ. The orientation distribution of Θ is described by the distribution function $\rho(\Theta)$. The immediate surroundings of a segment is a domain. All the domains $\wp$ have equal mechanical properties. The projection length of a chain is the length of the chain along the fibre axis. The fibre strain is equal to the average relative increase of the projection length. The projection length of a chain at a fibre stress σ_f is given by

$$L = L_c\langle[1 + \varepsilon_c(\Theta, \sigma_f)]\cos\,\theta(\Theta, \sigma_f)\rangle. \quad (1)$$

and thus the fibre strain by

$$\varepsilon_f = \frac{L - L_0}{L_0}. \quad (2)$$

In order to incorporate the yield in the theory for the elastic extension of polymer fibres several concepts from the continuum mechanics will be introduced. The

deformation is described by the mapping φ, a schematic drawing of φ is presented in Fig. 2. The deformation gradient of φ is denoted by $\boldsymbol{F}$. The deformation gradient $\boldsymbol{F}$ can be uniquely decomposed in a symmetric tensor $\boldsymbol{I} + \boldsymbol{U}$, the right stretch tensor, and a rotation $\boldsymbol{R}$

$$\boldsymbol{F} = \boldsymbol{R}(\boldsymbol{I} + \boldsymbol{U}). \tag{3}$$

It is supposed that no pure rotation occurs, i.e. $\boldsymbol{R} = \boldsymbol{T}$, with $\boldsymbol{T}$ a shifter that parallel transports vectors emanating from X to vectors emanating from $\varphi(X)$. In this case it holds that $F^i_J = (I + U)^i_J$. The relation between the deformation gradient $\boldsymbol{F}$ and the orientation angle of the deformed domain is given by the equation

$$\tan(\theta - \Theta) = \frac{F^1_3}{F^3_3}. \tag{4}$$

The elastic properties of a domain are defined by the relation between the elastic energy W and the deformation. For the analysis of the elastic extension of the fibre the form

$$W = \frac{1}{2} E^{IJKL} \varepsilon_{IJ} \varepsilon_{KL} \tag{5}$$

is chosen, with $\varepsilon_{IJ} = U_{IJ} + U_{IK}U_{KJ}$ the Lagrangian or material strain tensor. The stress–strain relation for this energy function is given by

$$S^{IJ} = E^{IJKL} \varepsilon_{KL}. \tag{6}$$

with $\boldsymbol{S}$ the second Piola stress tensor

$$\boldsymbol{S}^{IJ} = J(F^{-1})^I_i (F^{-1})^J_j \boldsymbol{\sigma}^{ij}. \tag{7}$$

J is the Jacobian of $\boldsymbol{F}$, and σ the Cauchy stress. It is supposed that the series assumption for the stress can be applied. This is equivalent to the assumption that the stress in the fibre is homogeneous and equal to the applied stress σ_f. Eqs. (1), (2) and (6), in conjunction with the series assumption, are the basic equations for the continuous chain model. In order to describe the yield properties of the fibre the stress–strain relation (6) is extended with a simple, semi-empiric yield condition.

For the description of the stress vs. strain curve of the fibre including yield it is supposed that all domains, in addition to equal elastic properties, have equal yield properties as well. It has been proposed by Northolt and Baltussen [14] that the yield of the fibre must be attributed to a local permanent shear deformation, i.e. a shear deformation of the domain. A permanent deformation implies that after application of a certain stress the shape of the domain in the unloaded state is changed. The undeformed domain is transformed to a new domain with a new unloaded shape. Due to the plastic deformation the direction of the chain axis changes permanently. It is assumed that the elastic properties of the permanently deformed domain, with respect to the direction of the chain axis of the permanently deformed domain, are equal to the elastic properties of the original domain.

2.2. The plastic deformation of a domain

The total deformation tensor of the domain is written as the product of the elastic and the inelastic deformation gradient

$$\boldsymbol{F} = \boldsymbol{F}_e \boldsymbol{F}_p. \tag{8}$$

The elastic properties of the plastically deformed domain are characterized by the angle $\Theta - \Delta\Theta_p$. The elastic part of the deformation is described by the equations for the elastic deformation of a domain at an angle $\Theta - \Delta\Theta_p$. Firstly the plastic deformation of the domain will be considered.

It is improbable that the plastic deformation of a domain of a polymer fibre is pure shear deformation, because, in second order, pure shear deformation causes an extension of the polymer chain as well: $\varepsilon_c = \frac{1}{2} U_{13}U_{31}$. Therefore, the permanent deformation should be a simple shear deformation. In Fig. 3 a pure shear deformation is compared with a simple shear deformation. It is noted that the simple shear deformation in Fig. 3 is a combination of a pure deformation and a rotation. Next the Cauchy–Green deformation tensor and the right stretch tensor associated to the simple shear deformation are calculated.

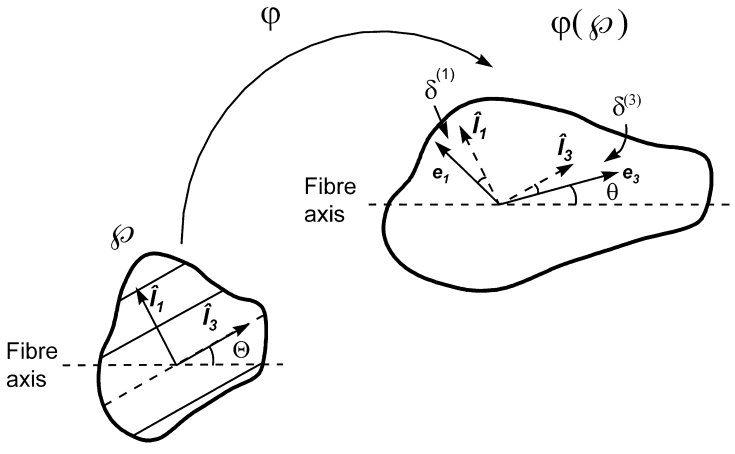

Fig. 2. Schematic drawing of the deformation.

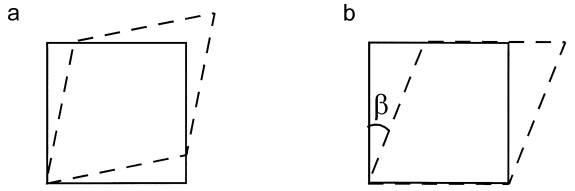

Fig. 3. A pure shear deformation (a) compared with a simple shear deformation (b). In case of pure shear the chain is extended, in case of simple shear it is not.

First the simple shear deformation will be analysed. A simple shear deformation is described by the deformation tensor

$$\boldsymbol{F} = \begin{bmatrix} 1 & 0 \\ \kappa & 1 \end{bmatrix}. \tag{9}$$

The parameter κ is equal to the tangent of the shear angle β. It is assumed that the permanent deformation is a pure deformation, just like the elastic deformation. This implies that no permanent rigid rotation of the domain occurs. As $\boldsymbol{F}$ is not symmetric it can be decomposed into a rotation and a symmetric tensor describing the deformation. The symmetric part of the decomposition of $\boldsymbol{F}$ is the right stretch tensor $\boldsymbol{I} + \boldsymbol{U}$ which is equal to the square root of the right Cauchy–Green deformation tensor $\boldsymbol{C} = \boldsymbol{F}^{\mathrm{T}}\boldsymbol{F}$

$$C = \begin{bmatrix} 1 + \kappa^2 & \kappa \\ \kappa & 1 \end{bmatrix}. \tag{10}$$

The right stretch tensor is given by

$$I + U = \sqrt{C} = \begin{bmatrix} \dfrac{1 + \sin^2 \alpha}{\cos \alpha} & \sin \alpha \\ \sin \alpha & \cos \alpha \end{bmatrix}, \tag{11}$$

with $2 \tan \alpha = \kappa$.

As we assumed that permanent deformation of the domain is simple shear deformation and that it is symmetric, it is described by Eq. (11) with $\kappa = \kappa_{\mathrm{p}}$. It is assumed that the parameter κ_{p} is a function of the elastic deformation. So, there is a relation between κ_{p} and an appropriate stress or strain measure describing the elastic deformation. In this paper a relation between κ_{p} and the components of $\boldsymbol{C}_{\mathrm{e}}$ is assumed. Further it is assumed that the plastic simple shear deformation is only related to the elastic simple shear deformation of the domain. Up to a certain value of the elastic deformation no plastic deformation occurs. Summarizing this results in two conditions:

- Permanent shear deformation is a function of the components of the right Cauchy–Green tensor of the elastic deformation $\boldsymbol{C}_{\mathrm{e}}$.
- In the case of an elastic simple shear deformation with shear parameter κ_{e} the plastic deformation is a simple shear deformation with κ_{p}, which is only a function of $\kappa_{\mathrm{e}} - \kappa_{\mathrm{y}}$, where κ_{y} is the critical yield strain.

For an elastic simple shear deformation we note that κ_{e} is equal to $\tan \beta$, with β the shear angle, see Fig. 3. The angle β can be calculated from the directions of the unit vector $\hat{\imath}_3$ in the direction of the chain and the unit vector $\hat{\imath}_1$ perpendicular to the chain after the deformation

$$\beta = \delta^{(3)} - \delta^{(1)}, \tag{12}$$

with $\delta^{(3)}$ the angle between $\boldsymbol{T}(\hat{\boldsymbol{I}}_3)$ and $\boldsymbol{F}(\hat{\boldsymbol{I}}_3)$ and $\delta^{(1)}$ the angle between $\boldsymbol{T}(\hat{\boldsymbol{I}}_1)$ and $\boldsymbol{F}(\hat{\boldsymbol{I}}_1)$ see Fig. 2. The definition of κ_{e} can simply be generalized using Eq. (12) for β. Consider an elastic deformation $\boldsymbol{F} = \boldsymbol{T}(\boldsymbol{I} + \boldsymbol{U})$ with

$$\boldsymbol{I} + \boldsymbol{U} = \begin{bmatrix} 1 + U_{11} & U_{13} \\ U_{31} & 1 + U_{33} \end{bmatrix}, \tag{13}$$

with $U_{13} = U_{31}$. The angle $\delta^{(1)}$ is given by

$$\tan \delta^{(1)} = -\frac{U_{13}}{1 + U_{11}} \tag{14}$$

and $\delta^{(3)}$ by

$$\tan \delta^{(3)} = \frac{U_{13}}{1 + U_{33}}. \tag{15}$$

Again the total shear angle is given by $\beta = \delta^{(3)} - \delta^{(1)}$. The value κ_e for an elastic deformation $\boldsymbol{I} + \boldsymbol{U}$ is defined as

$$\kappa_{\mathrm{e}} = \tan \beta. \tag{16}$$

By this definition κ_{e} is only a function of the pure deformation, because κ_{e} can be expressed in the components of $\boldsymbol{C}$

$$\kappa_{\mathrm{e}} = \sqrt{C_{22}}\frac{C_{13}}{J}, \tag{17}$$

with $\boldsymbol{J}$ the determinant of $\boldsymbol{I} + \boldsymbol{U}$. By this definition κ_{e} is independent of the change of the length of a line segment parallel or perpendicular to the chain segment due to the deformation. It is assumed that κ_{p} is a function of $\kappa_{\mathrm{e}} - \kappa_{\mathrm{y}}$ with κ_{y} the critical yield strain

$$\kappa_{\mathrm{p}} = P(|\kappa_{\mathrm{e}}| - \kappa_{\mathrm{y}}), \tag{18}$$

with $\boldsymbol{P}$ a suitable function describing the yield properties of a single domain. Analogous to the analysis of the elastic deformation the equations for the yielding fibre are calculated in the second order of the components of $\boldsymbol{U}$. The second order approximation of Eq. (18) is given by

$$\kappa_{\mathrm{p}} \approx P(|2U_{13}| - \kappa_y). \tag{19}$$

The permanent deformation of the domain is given by

$$\boldsymbol{F}_{\mathrm{p}} = \begin{bmatrix} \dfrac{1 + \sin^2 \alpha_{\mathrm{p}}}{\cos \alpha_{\mathrm{p}}} & \sin \alpha_{\mathrm{p}} \\ \sin \alpha_{\mathrm{p}} & \cos \alpha_{\mathrm{p}} \end{bmatrix}, \tag{20}$$

with $2 \tan \alpha_{\mathrm{p}} = \kappa_{\mathrm{p}}$. Due to the permanent deformation the orientation of the chain segment changes. The load free orientation angle of the permanently deformed domain is given by $\boldsymbol{\Theta}_{\mathrm{p}} = \boldsymbol{\Theta} + \Delta\boldsymbol{\Theta}_{\mathrm{p}}$. Using Eq. (4) the rotation

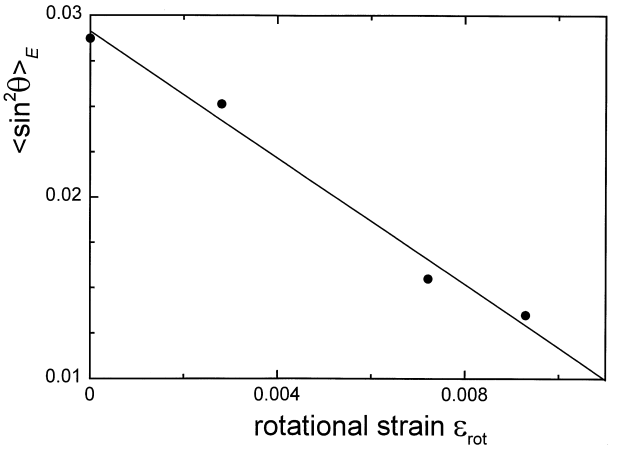

Fig. 4. The strain of a PpPTA fibre vs. the orientation parameter $\langle \sin^2 \theta \rangle_E$ measured by X-ray diffraction.

angle $\Delta\Theta_p$ follows from $\boldsymbol{F}_p$ by

$$\tan \Delta\Theta_p = \tan \alpha_p = \frac{1}{2}\kappa_p. \tag{21}$$

Combination of Eqs. (21) and (19) for κ_p yields for the permanent rotation of the chain segment the formula

$$\tan \Delta\Theta_p = \frac{1}{2}P\Big(|2U_{13}| - \kappa_y\Big). \tag{22}$$

The total deformation of the domain follows from the product of the plastic deformation $\boldsymbol{F}_p$ and the elastic deformation $\boldsymbol{F}_e$ of a domain under an angle Θ_p.

2.3. The stress vs. strain curve of a yielding fibre

In Ref. [12] a second order approximation for the elastic stress vs. strain curve of a fibre of linear polymer has been derived. The elastic strain of a fibre is given by

$$\varepsilon_f = \frac{1}{\langle \cos \Theta \rangle} \times \left[\frac{\sigma_f \langle \cos\theta [1 - \sin^2\theta (1 + \nu_{13} + 2\cos^2\theta \frac{\sigma_f}{2g})] \rangle}{e_c} + \langle \cos\theta \rangle - \langle \cos\Theta \rangle \right] \tag{23}$$

with the formula

$$\tan(\theta - \Theta) = -\frac{\sigma_f}{2g} \frac{\left(1 - \frac{\nu_{12}\sigma_f}{e_1}\sin^2\theta\right)}{\left[1 + \frac{1}{2}\frac{\sigma_f}{e_1}\sin^2\theta + \frac{\sigma_f}{g}\sin^2\theta\right]} \sin\theta\cos\theta \tag{24}$$

for the elastic rotation of the chain segment. The sonic modulus of a fibre is given by the equation

$$\frac{1}{E_f} = \frac{1}{e_c} + \frac{1}{2g\langle\cos\theta\rangle} \times \left\langle \sin^2\theta \cos\theta \left[\frac{1 - \sigma_f \sin^2\theta \left[\frac{2\nu_{12}}{e_1} + \frac{1}{2e_1} + \frac{1}{g} \right]}{1 + \frac{\sigma_f}{2g} + \frac{\sigma_f}{2e_1}\sin^2\theta} - \frac{2g(1+\nu_{13}) + 2\sigma_f(3-\nu_{13})\cos^2\theta}{e_c} \right] \right\rangle. \tag{25}$$

As we assume that the elastic properties of the permanently deformed domain are equal to the elastic properties of the original domain, Eqs. (23) and (25) for the strain and the sonic modulus can be used for the permanently deformed fibre. Eq. (24) for the orientation angle of the

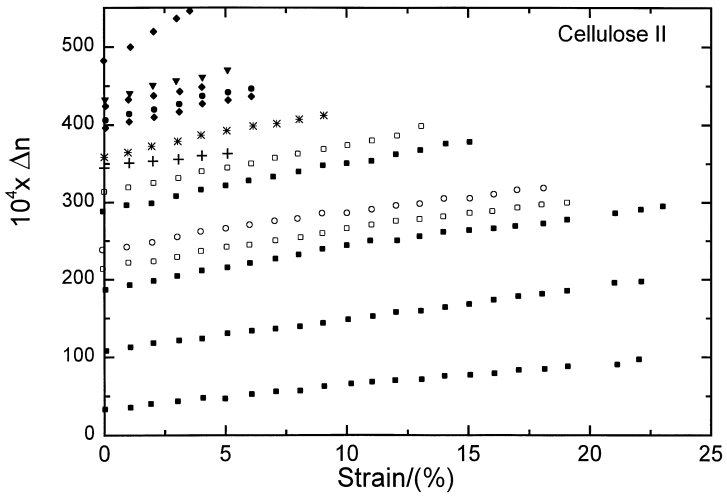

Fig. 5. The birefringence vs. the strain of a collection of cellulose yarns measured by de Vries [16].

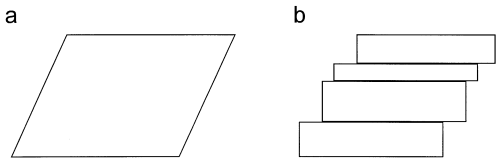

Fig. 6. A domain of a fibre showing continuous yield (a) compared with a domain with slip planes (b).

chain segment can be used as well using the new load free orientation angle $\Theta_p = \Theta + \Delta\Theta_p$ instead of Θ. Substitution of Θ by Θ_p in the left hand side of Eq. (24) yields

$$\tan(\theta - \Theta_p) = \tan((\theta - \Theta) - \Delta\Theta)) = \frac{\tan(\theta - \Theta) - \tan\Delta\Theta_p}{1 + \tan(\theta - \Theta)\tan\Delta\Theta_p} \quad (26)$$

In second order of $\boldsymbol{U}$ Eq. (26) can be approximated by

$$\tan((\theta - \Theta) - \Delta\Theta_p)) = \tan(\theta - \Theta) - \tan\Delta\Theta_p \quad (27)$$

Combination of Eqs. (22), (24) and (27) yields, for the orientation angle of the yielding domain, the set of equations

$$\tan(\theta - \Theta) \approx U_{13} + \frac{1}{2}P(|2U_{13}| - \kappa_y) \quad (28)$$

$$U_{13} \approx -\frac{\sigma_f}{2g}\frac{\left(\frac{1 - \nu_{12}\sigma_f}{e_1}\sin^2\theta\right)}{\left[1 + \frac{1}{2}\frac{\sigma_f}{e_1}\sin^2\theta + \frac{\sigma_f}{g}\sin^2\theta\right]}\sin\theta\cos\theta$$

Eq. (28) in combination with Eq. (23), describes the stress vs. strain curve of a yielding fibre, Eq. (28) in combination with Eq. (25) describes the sonic modulus vs. stress curve. In case of highly oriented fibres and moderate stress Eq. (28) can be approximated by the simple equation

$$\tan(\theta - \Theta) \approx U_{13} + \frac{1}{2}P(|2U_{13}| - \kappa_y) \quad (29)$$

$$U_{13} \approx -\frac{\sigma_f}{2g}\sin\theta\cos\theta.$$

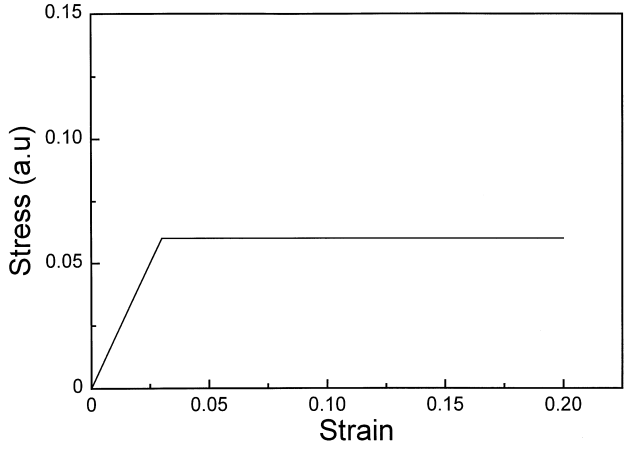

Fig. 7. The stress vs. strain curve of an ideal plastic domain.

3. The nature of yield

For the quantitative description of the plastic shear of a domain no physical model is available yet, therefore a reasonable guess must be made. First some observations about the yield are discussed. In the derivation of the equations for the fibre with yield it has been supposed that:

1. The deformation of the fibre with yield can be described by the continuous chain model.
2. The yield of the fibre is due to simple shear deformation of the domains.
3. All domains have equal yield properties. This implies that the yield strain is a spatially homogeneous quantity, which varies continuously as a function of the applied stress and the initial load free orientation angle of the chain segment.

The continuous chain model assumes that only shear deformation and extension of the chain contribute to extension of the fibre. Because of the rigidity of the chains in the domain the only possible permanent deformation of the domain is a simple shear deformation of the domains. The rotational strain of the fibre of the fibre is defined by [12]

$$\varepsilon_{rot} = \varepsilon_f - \frac{\sigma_f}{e_c} \approx \frac{\langle\cos\theta\rangle - \langle\cos\Theta\rangle}{\langle\cos\Theta\rangle}. \quad (30)$$

Eq. (30) shows that, according to the continuous chain model, the rotational strain should be a smooth function of the orientation distribution. Fig. 4 shows the orientation parameter $\langle\sin^2\theta\rangle_E$ measured by X-ray diffraction vs. ϵ_{rot}

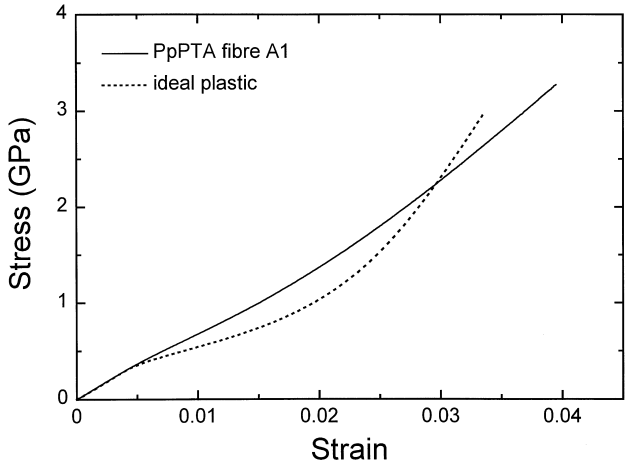

Fig. 8. The stress vs. strain curve calculated with the ideal plastic yield criterion compared with the stress vs. strain curve of the PpPTA fibre A1.

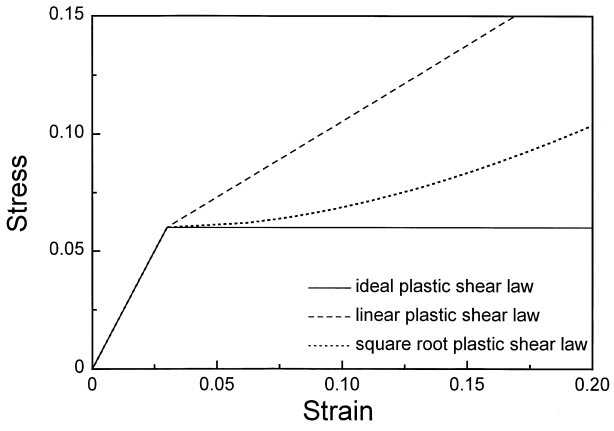

Fig. 9. The deformation behaviour of the domain according to the proposed plastic shear laws.

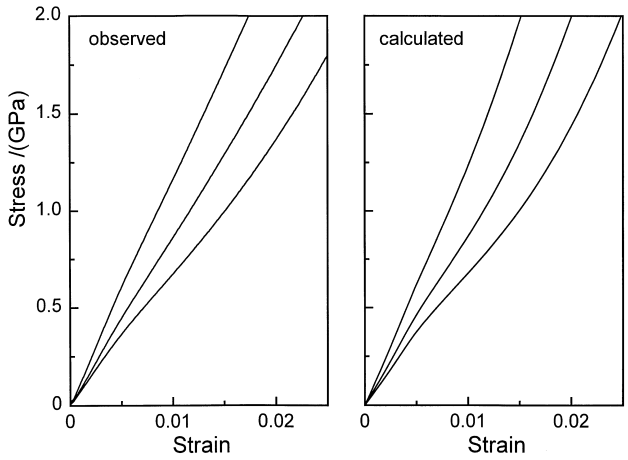

Fig. 10. The observed stress strain curves (a) of three PpPTA fibres compared with the calculated curves.

for a PpPTA fibre. In the yield region no different behaviour is observed, which confirms the assumption that a single deformation mechanism governs the deformation below and above the yield point. De Vries performed an extensive investigation into the birefringence of cellulose fibres during extension [16]. The birefringence is linearly related to the orientation parameter $\langle \sin^2 \theta \rangle$. His results, which are reproduced in Fig. 5, show that a linear relation is found between the orientation parameter $\langle \sin^2 \theta \rangle$ and the strain for a large collection of fibres with very different values for the initial modulus. No abrupt change of the slope of $\langle \sin^2 \theta \rangle$ vs. the strain can be observed at the yield point in the range of 0.005–0.02 strain. These measurements also confirm that the deformation below and above the yield stress is governed by shear deformation of the domains.

The second assumption might be a simplification of the yield process on molecular level. In polycrystalline materials plastic deformation occurs along slip planes, so it has a discrete character. The mechanism for plastic deformation is governed by dislocations in the material. The cases of homogeneous yield and yielding along slip planes have been depicted schematically in Fig. 6. Considering the para-crystalline structure of PpPTA fibres, the plastic deformation process is probably similar to plastic deformation in polycrystalline materials. In fibres of an amorphous polymer without packing coherence in the direction perpendicular to the direction of the chain yield deformation may be more homogeneous. The same holds for a semi-crystalline fibre with amorphous regions. The macroscopic similarity of the yield behaviour of amorphous, semi-crystalline and para-crystalline fibres indicates that the yield process in all these materials occurs in a similar way. However, the discussion about the details of molecular processes during yield deformation has not been finished yet. Argon and coworkers showed that the plastic deformation of amorphous polymers is strongly hindered by the rigid chains in the material [7]. He concludes that the restricted mobility of the molecules makes the motion of dislocations far removed from reality.

The second assumption excludes the occurrence of a neck. In a neck strong localisation of plastic deformation occurs. Without necking the plastic deformation will be distributed homogeneously over the fibre.

From these considerations it is concluded that the assumption, that all domains have equal yield properties, may be a simplification of the yielding process, especially in the case of para-crystalline materials. However, the distribution of the discrete yield transformations at molecular level is likely to be dense enough to justify the use of a continuum model for the calculation of the stress vs. strain curve of a yielding fibre. The value of the yield strain is the average of the shear yield displacements in a small region. From this description of the yield deformation it becomes plausible that the elastic properties of the permanently deformed domain are equal to the elastic properties of the undeformed domain. In para-crystalline polymers and in the crystalline regions of semi-crystalline polymers permanent deformation occurs along slip planes. The structure of the domains does not change, neither do the elastic properties. In amorphous polymers, or in the amorphous regions of semi-crystalline polymers the lateral ordering is very poor, and will not be effected by plastic shear displacements very much.

Table 1
The parameters for the calculated stress vs. strain curve

	PpPTA		PET	
Domain parameters				
g	1.8–2.4 GPa [13]		1.0–1.5 GPa [13]	
κ_y	0.04–0.07 [14]		0.04–0.07 [14]	
p	Depends on the choice for P			
Orientation distribution				
	Gauss	Affine	Gauss	Affine
Parameters	z	λ	z	λ

Table 2
The parameters used for the calculation of the stress vs. strain curves of the PpPTA fibres

Fibre	E_0 (GPa)	e_c (GPa)[a]	e_1 (GPa) [13]	ν_{12} [13]	ν_{13} [13]	g (GPa)	κ_y	p	Distribution
A1	71	220	5.5	0.65	0.3	2	0.06	3	Gauss
A2	89	220	5.5	0.65	0.3	2	0.06	3	Gauss
A3	124	220	5.5	0.65	0.3	2	0.06	3	Gauss

[a] Northolt and Sikkema [20], Barton [21]: 240 GPa.

4. The yield function *P*

A domain is symmetric with respect to reflection in a plane perpendicular to the chain segment. As the yield function P must have the same symmetry it holds that $P(-\kappa_e) = -P(\kappa_e)$. At the yield point the critical yield stress is exceeded along certain slip planes, probably due to the failure of secondary bonds. With respect to this yield process, a simple model for the yield of a domain is ideal plastic behaviour. This implies that above the critical yield strain κ_y all additional deformation is plastic. The corresponding stress vs. strain curve of the domain in simple shear has been depicted in Fig. 7. For this "maximum elastic shear strain" plastic shear law, the function P is multiple valued at $\kappa_e = \kappa_y$. Nevertheless this gives a stable solution for the stress vs. strain curve of the fibre. The plastic shear deformation causes a decrease of the orientation angle θ and thus a decrease of the resolved shear stress on the domain. At a certain value of the applied tensile stress the plastic shear deformation is determined by the condition that the elastic shear strain is exactly equal to κ_y

$$\begin{aligned} \tan(\theta - \Theta) &= U_{13} \quad |U_{13}| < \frac{1}{2}\kappa_y \\ U_{13} &= \pm\frac{1}{2}\kappa_y \qquad \text{else} \end{aligned} \tag{31}$$

U_{13} is given by Eq. (28). If a tensile stress is applied to the fibre U_{13} will be negative. The calculated stress vs. strain curve according to this very simple formula has been drawn in Fig. 8. The calculated curve has been compared to the observed stress vs. strain curve of the PpPTA fibre A1. The calculated curve shows the typical features of the experimental curve, i.e. the initial elastic part, the yielding at about 0.005 strain continuing in a concave curve up to failure. However, it is obvious that the yield of the calculated curve is much too large. This indicates that strain hardening occurs, and thus the yield resistance increases with increasing plastic deformation. Such a strain hardening is very common in crystalline materials and can be due to limited mobility of dislocations [17].

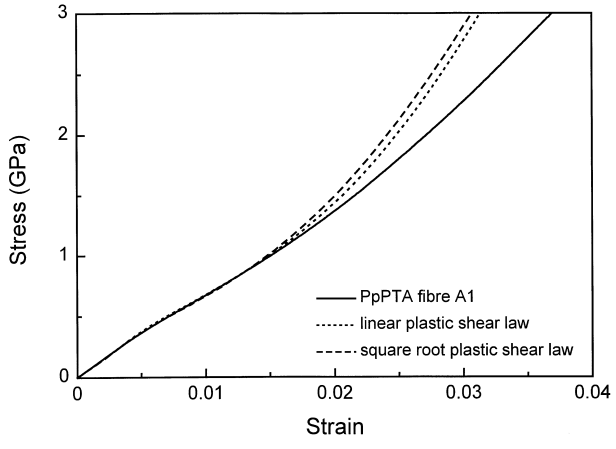

Fig. 11. The square root plastic law compared with the linear plastic shear law for the PpPTA fibre A1.

For the modelling of the strain hardening two plastic shear laws will be studied. It should be emphasized that these plastic shear laws are phenomenological relations. They are chosen because they describe the stress vs. strain curves rather successfully. The "linear" shear yield law supposes that above the yield point, the resistance to yielding increases linearly with the yield strain

$$\begin{aligned} \tan\Delta\Theta_p &= 0 \qquad\qquad |U_{13}| \le \frac{1}{2}\kappa_y \\ \tan\Delta\Theta_p &= \frac{1}{2}p\cdot(2U_{13} + \kappa_y) \quad |U_{13}| > \frac{1}{2}\kappa_y \end{aligned} \tag{32}$$

The parameter p must be adjusted for each curve and U_{13} is supposed to be negative again. It will be shown that the linear plastic shear law is useful for the description of the stress vs. strain curves of PpPTA fibres. For the stress vs. strain curves of PET fibres a good agreement with the experimental curve can be achieved by a "square root" shear yield law

$$\begin{aligned} \tan\Delta\Theta_p &= 0 \qquad\qquad |U_{13}| \le \frac{1}{2}\kappa_y \\ \tan\Delta\Theta_p &= \frac{1}{2}p\cdot\sqrt{-2U_{13} - \kappa_y} \quad |U_{13}| > \frac{1}{2}\kappa_y \end{aligned} \tag{33}$$

The plastic shear law defines the deformation behaviour of the domain. In Fig. 9 the deformation of the domain has been drawn for the three yield criteria.

5. Results and discussion

5.1. The stress vs. strain curve

For a realistic comparison of the calculated stress vs. strain curves with the experimental curves the parameters for the calculated curve must be chosen carefully. In Table 1

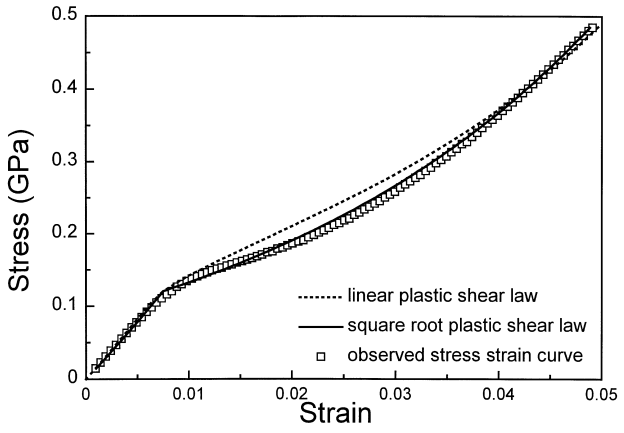

Fig. 12. The experimental stress vs. strain curve of the PpPTA fibre 1125T compared with the calculated curves using the linear and the square root plastic shear laws.

the adjustable parameters are listed together with the possible choices for PpPTA and PET fibres.

In addition to the mechanical parameters characterizing the domain, the orientation distribution of the fibre has a large influence on the stress vs. strain curve of the fibre. The Gaussian distribution is given by

$$\rho(\Theta) = \exp\left[-\frac{\sin^2 \Theta}{z^2}\right]. \tag{34}$$

A Gaussian distribution can be expected if the orientation distribution is due to a thermodynamic equilibrium, e.g. in case of highly oriented aramid fibres [18]. An affine distribution, which is given by

$$\rho(\theta) = \left(\frac{\lambda^2}{\cos^2 \Theta + \lambda^3 \sin^2 \Theta}\right)^{3/2} \tag{35}$$

can be expected from a non-equilibrium drawing process, such as a neck occurring in the high speed spinning process for PET fibres [14,19].

Stress vs. strain curves using the linear plastic shear law, see Eq. (32), were calculated for a set of aramid fibres. The experimental curves are plotted in Fig. 10(a) and the calculated curves have been plotted in Fig. 10(b). The shear modulus g is the average value calculated from the modulus vs. the strain curves of PpPTA fibres, using the technique described in Ref. [11]. The yield strain κ_y and the yield parameter p are determined by comparison with the experimental stress vs. strain curves. The complete set of parameters used for the calculated curves is given in Table 2.

From Fig. 10 it can be concluded that the linear plastic shear law gives a satisfactory description of the stress vs. strain curves of the tested aramid fibres. For higher tensions the observed strain tends to be higher than the calculated strain. This can be due to several causes, the most important ones have been identified in Ref. [13]. Especially at high tensile stress there will be a small contribution of chain slip to the total extension or the fibre, in addition to the shear deformation of the domains. At high tensile stress also the quadratic form for the stored energy function will be too simple an approximation for the description of the elastic response of the fibre. In Fig. 11 the linear plastic shear law is compared with the square root plastic shear law. For the curve calculated according to the square root plastic shear law a value of $p = 0.6$ was used. Although the differences are rather small it can be concluded that the linear plastic shear law gives a better fit to the observed stress vs. strain curve.

For the PET fibre Diolen 1125T the linear plastic shear law has been compared with the square root plastic shear law as well. The result has been plotted in Fig. 12. The parameters used for the calculated curves have been listed in Table 3.

The main characteristics of the experimental curves can be reproduced by using the linear plastic shear law, but examination of the yield region demonstrates that the linear plastic shear law does not describe the characteristic “dip” just above the yield point. This typical feature of the stress vs. strain curve of PET fibres is reproduced better by the square root plastic shear law. From this result it can be concluded that the strain hardening in highly oriented PpPTA fibres initiates immediately above the yield point, while in oriented PET fibres the strain hardening begins only after a certain plastic shear deformation, see Fig. 9. Apparently the less oriented and less crystalline domains in PET fibres yield more easily than the para-crystalline domains of the aramid fibres.

5.2. The stress vs. strain and sonic modulus vs. strain curves

In the previous section the calculated stress vs. strain curve has been compared with the experimental curves. With Eqs. (23)–(25) the strain and the sonic modulus as a function of the applied stress can be calculated for a single fibre. In this section these equations are fitted simultaneously to both the sonic modulus vs. strain curve and the stress vs. strain curve of a selection of PpPTA and PET fibres. The yield of PpPTA fibres is described by the

Table 3
The parameters which have been used for the calculation of the stress vs. strain curve strain of the PET fibre Diolen 1125T using the linear and the square root plastic shear law

Shear law	E_0 (GPa)	e_c (GPa) [13]	e_1 (GPa) [13]	ν_{12} [13]	ν_{13} [13]	g (GPa)	κ_y	p	Distribution
Lin.	14	125	3	0.65	0.3	1.1	0.05	3.5	affine
Sq. rt.	16	125	3	0.65	0.3	1.1	0.054	1.1	affine

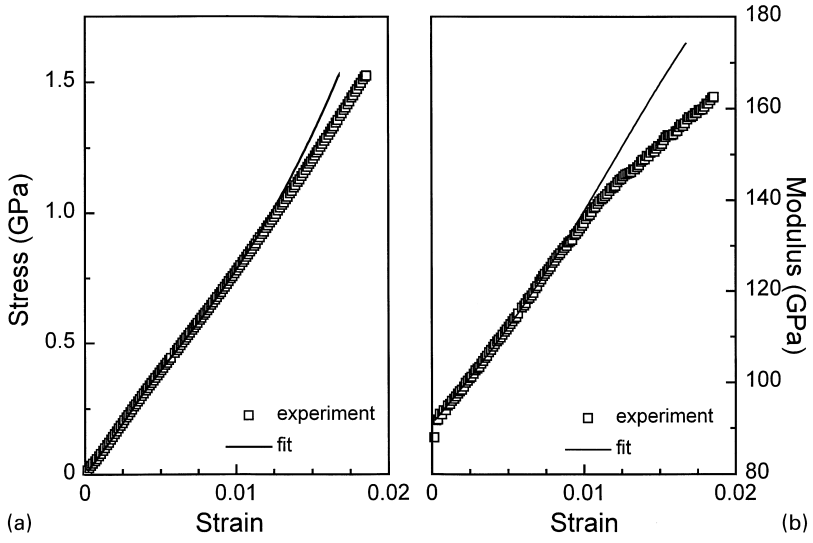

Fig. 13. The simultaneous fit of (a) the stress vs. strain and (b) the modulus vs. strain curve of the PpPTA fibre Twaron 1000.

linear plastic shear law and the yield of PET fibres is described by the square root plastic shear law.

Before explaining the fit procedure the number of independent parameters is discussed. Using a single parameter orientation distribution, like a Gaussian or an affine distribution, the number of adjustable parameters in the equations is four, i.e. g, (z or λ), κ_y and p. These four parameters are linked to four independent features of the stress vs. strain curve. The shear modulus g in combination with z or λ determine the sonic modulus and the slope of the sonic modulus vs. the strain curve. The yield point parameter κ_y is uniquely determined by the yield point and p determines the depth of the yield. As these are independent features of the stress vs. strain curve, four variables is the minimum number necessary to fit these four features of the experimental curves. If an experimental value for the width of the orientation distribution is available, e.g. calculated from the birefringence of the fibre, a fifth experimental variable is available and thus five independent parameters can be determined. In this case the shape of the orientation distribution can be fitted with, for example, a Pearson VII function [22]. For the description of the sonic modulus and the strain as a function of the stress of these fibres only a Gaussian or an affine orientation distribution will be used.

The initial value for the shear modulus g and the width z of the orientation distribution are determined from the sonic modulus vs. strain curve using the method described in Ref. [13]. In the case of aramid fibres, the sonic modulus at zero stress is almost equal to the initial modulus of the stress vs. strain curve. For PET fibres the initial modulus of the stress vs. strain curve is somewhat lower, which is probably due to the larger viscoelasticity of these fibres. Therefore the stress vs. strain curve is described with the help of a shear modulus g_m which is slightly lower than the shear modulus g of the sonic modulus vs. strain curve. In formula (28) for the orientation angle θ of the chain segment, the value g_m is used, because the value of θ determines the value of the calculated strain, see Eq. (23). In formula (25) for the sonic modulus the sonic value g is used. With constant values for g and z calculated from the sonic modulus vs. strain curve, the values of the parameters p, κ_y and g_m are determined from the stress vs. strain curve. The final values for the shear modulus and z are obtained by fitting the sonic modulus vs. stress curve, with the value of the sonic modulus as a constraint.

The sonic modulus and the strain of a Twaron 1000 yarn have been fitted using a Gaussian orientation distribution. The results are presented in Fig. 13 and the parameters derived from the fit procedure are listed in Table 4.

The low value of g_m is due to fact that the modulus of the stress vs. strain curve of a bundle is always somewhat lower than the modulus of the individual filaments or the sonic modulus. The measurement was performed on a bundle because the sonic modulus cannot be accurately measured on single filaments.

The sonic modulus and strain of Diolen 1125T were fit by using an affine orientation distribution. For the fit of the sonic modulus and strain of Diolen 147S a Gaussian

Table 4
The parameters used for the calculation of the sonic modulus and the strain as a function of the stress of the Twaron 1000 fibre

Fibre	E_0 (GPa)	g (GPa)	g_m (GPa)	κ_y	p	z	$\langle \sin^2 \theta \rangle$ $E_{son} - \varepsilon$	$\langle \sin^2 \theta \rangle$ *X-ray*
Twaron 1000	91.6	2.0	1.42	0.057	1.7	0.16	0.0263	0.024

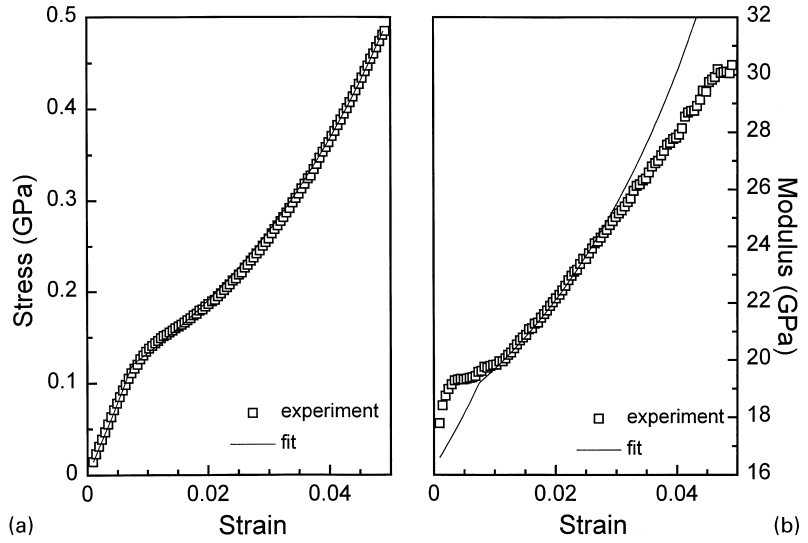

Fig. 14. The simultaneous fit of (a) the stress vs. strain and (b) the modulus vs. strain curve of the PET fibre Diolen 1125T.

orientation distribution was used. The calculated curves are compared with the experimental ones in Figs. 14 and 15. The parameters used for the calculated curves have been listed in Table 5.

Figs. 13–15 show that the curves of sonic modulus and strain vs. applied tensile stress of both PpPTA and PET fibres can be described simultaneously by the proposed equations for fibres with yield. A value for the width z of the orientation distribution was determined by fitting these curves. Using this value the orientation parameters can be calculated. In Table 3 the value for $\langle \sin^2 \theta \rangle$ determined by the fit of the mechanical data of the Twaron 1000 fibre has been compared with the value measured by X-ray diffraction. A good agreement between the two values has been found. It results from their birefringence that both PET fibres have the same value for $\langle \sin^2 \theta \rangle$. The errors on the values of $\langle \sin^2 \theta \rangle$ determined by the fit procedure are not known very well because not all parameters were varied simultaneously, and because no statistical data from a large number of experiments is available. The estimated error is in the order of 5%. So it can be concluded that, also for the PET fibres, the values for $\langle \sin^2 \theta \rangle$ calculated from the mechanical data are in good agreement with the values calculated from the birefringence of the yarn.

In conclusion it has been demonstrated that the essential features of the observed tensile curve and the sonic modulus during tensile extension can be described by the use of the continuous chain model in combination with a simple plastic shear law for plastic deformation of the domain.

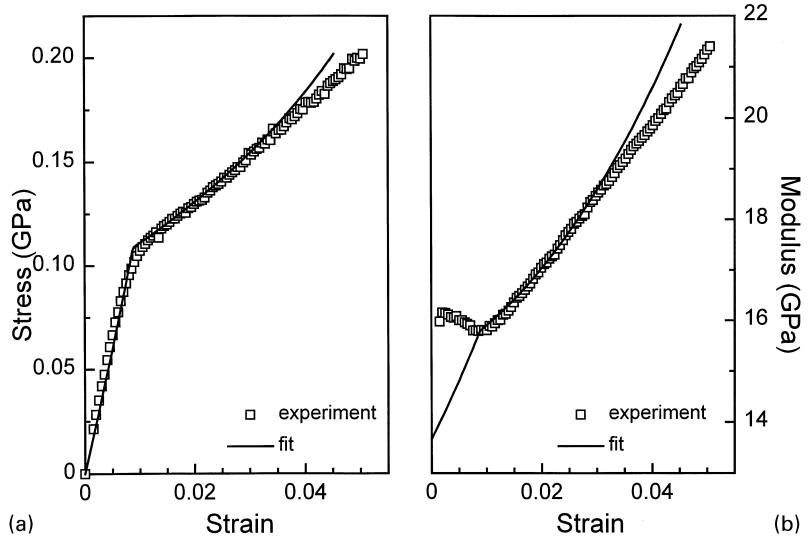

Fig. 15. The simultaneous fit of (a) the stress vs. strain and (b) the modulus vs. strain curve of the PET fibre Diolen 174T.

Table 5
The parameters used for the calculation of the sonic modulus and the strain as a function of the stress of the PET fibres. The value for $\langle \sin^2 \theta \rangle \Delta_n$ has been calculated using a value of 0.25 for the maximum value of Δn

Fibre	E_0 (GPa)	g (GPa)	g_m (GPa)	κ_y	p	$\frac{\langle \sin^2 \theta \rangle_E}{E_{son} - \varepsilon}$	$\frac{\langle \sin^2 \theta \rangle}{E_{son} - \varepsilon}$	$\langle \sin^2 \theta \rangle_{\Delta n}$
Diolen 174S	14	1.2	1.0	0.049	2.3	0.1641	0.192	0.186
Diolen 1125T	17	1.1	1.0	0.054	1.1	0.1217	0.185	0.186

Acknowledgements

We thank Mrs. B. Schaffers Korff for doing the stress vs. strain measurements and Prof. I.M. Ward and Prof. F. Tuinstra for critical reading of the manuscript.

References

[1] Ward IM. Mechanical properties of solid polymers. Chichester: Wiley, 1971.
[2] Zaukelies DA. J Appl Phys 1962;33:2797.
[3] Haward RN, Thackray G. Proc Roy Soc A 1968;302:453.
[4] Young RJ. Phil Mag 1974;30:85.
[5] Young RJ. Mater Forum 1988;11:210.
[6] Mott PH, Argon AS, Suter UW. Phil Mag A 1993;4:931.
[7] Argon AS, Bulatov VV, Mott PH, Suter UW. J Rheol 1995;39:377.
[8] Tresca H. Compt Rend Acad Sci Paris 1864;59:754.
[9] Coulomb CA. Mém Math Phys 1773;7:343.
[10] Von Mises R. Göttinger Nachrichten, Math-Phys Klasse 1913, p. 582.
[11] Cottrell AH. Dislocations and plastic flow in crystals. Oxford: Clarendon Press, 1953 p. 4.
[12] Baltussen JJM, Northolt MG, Van der Hout R. J Rheol 1997;41:549.
[13] Baltussen JJM, Northolt MG. J Rheol 1997;41:575.
[14] Northolt MG, Baltussen JJM, Schaffers-Korff B. Polymer 1995;36:3485.
[15] Baltussen JJM, Northolt MG. Polym Bull 1996;36:125.
[16] de Vries H. On the elastic and optical properties of cellulose fibres, Doctoral Thesis, University of Delft, The Netherlands, 1953.
[17] Reed-Hill RE. Physical metallurgy principles. Princeton: Van Nostrand, 1967 p. 123.
[18] Picken S. Orientational order in aramid solutions, Doctoral Thesis, University of Utrecht, The Netherlands, 1990.
[19] Picken S. Personal communication, 1995.
[20] Northolt MG, Sikkema DJ. Adv Polym Sci 1990;98:119.
[21] Barton R. J Macromol Sci Phys (1985–1986) 1986;B24:119.
[22] Hall Jr. MM. J Appl Cryst 1977;10:66.